



“Gheorghe Asachi” Technical University of Iasi, Romania



---

## REMOVAL OF HEXAVALENT CHROMIUM USING TWO INNOVATIVE ADSORBENTS

Reda Abubeah<sup>1\*</sup>, Hossam Altaher<sup>2</sup>, Tarek E. Khalil<sup>3</sup>

<sup>1</sup>Department of Chemical Engineering, Faculty of Engineering, El-Minia University P.O. Box 6151, El-Minia, Egypt

<sup>2</sup>Department of Chemical Engineering Technology, Yanbu Industrial College P.O. Box 30436, Yanbu Industrial City, Saudi Arabia

<sup>3</sup>Chemistry Department, Faculty of Science, Alexandria University P.O. Box 426 Ibrahimia, Alexandria 21321, Egypt

---

### Abstract

Hexavalent chromium Cr(VI), a constituent of wastewater from many industries, is regulated by the Environmental Protection Agency (EPA) as one of the priority pollutants. Adsorption is an important technique that can be used for Cr(VI) removal from wastewater. The challenge in adsorption techniques is to find a cheap, widely available adsorbent that has a high adsorption capacity to Cr(VI). Dates stones (DS) and palm fiber (PF) are two agricultural wastes that are produced from palm trees. These adsorbent materials were tested in batch systems to investigate the different factors that may affect the adsorption process, e.g. adsorbent dose, initial adsorbate concentration, pH of aqueous solution and agitation time. Equilibrium models tested include Langmuir, Freundlich, Temkin and Dubinin-Radushkevich. Freundlich adsorption isotherm was found to best fit the experimental data. The maximum adsorption capacities obtained for DS and PF were 16 and 6 mg/g, respectively. Kinetic studies indicated that the adsorption of Cr(VI) on both DS and PF was fast in the first stage of the adsorption process. The equilibrium was reached in less than 2 h for both adsorption systems. The adsorption process was found to be second order with both adsorbent and adsorbate concentration to affect the adsorption process. Film diffusion and intraparticle diffusion models were found to simultaneously influence the adsorption. The adsorption process was found to be favorable and of physical nature.

*Key words:* adsorption, chromium (VI), dates stones, kinetics, palm fiber, thermodynamic

*Received:* August, 2013; *Revised final:* August, 2014; *Accepted:* September, 2014; *Published in final edited form:* July 2018

---

### 1. Introduction

The excessive industrial disposal of heavy metals represents a major source of pollution problems (Štrkalj et al., 2013). Chromium is heavily used in many industries like tanning of leather, cement manufacturing, dyeing of textile, electroplating, chromate preparation, pulp and paper, fertilizer, alloy and steel manufacturing, and colorants production. The wastewater from these industries contains chromium and its compounds in concentrations higher than the permissible limit.

Chromium has two oxidation states; hexavalent and trivalent. Chromium (VI) is 100-1000 times more toxic to organisms than Cr (III).

Chromium has many adverse effects on human beings like damage to liver, kidney, circulatory and nerve tissues (Blázquez et al., 2009; Hlihor et al., 2009; Natarajan and Nagarajan, 2010).

The treatment of wastewater containing chromium includes many physical and chemical methods like solvent extraction, reverse osmosis, cementation onto iron, electrocoagulation (Sadeghi et al., 2017), bioremoval (Fathima et al., 2017, Ghorbani and Younesi, 2016), floating electrochemical precipitation, ultra filtration, ion exchange, electro dialysis, chemical oxidation and reduction (Gheju and Balcu, 2011; Štrkalj et al., 2013). These conventional methods were found to be expensive and inefficient, especially when treating wastewater

---

\* Author to whom all correspondence should be addressed: e-mail: [redaabubeah@yahoo.com](mailto:redaabubeah@yahoo.com); Phone: + 966597454109; Fax: +96643920213

with low concentration of heavy metals. Another problem that must be taken into consideration is that some of these conventional methods produce chemical or biological toxic sludge. For example, the chemical precipitation produces large amounts of sludge that must be disposed of. Another drawback of most of these methods is the difficulty of recovery of the metals from these sludges (Attia et al., 2010).

Adsorption process represents an excellent alternative for treatment of wastewater containing heavy metal. Some important advantages of the adsorption technique are low initial cost, low operating cost, flexibility and simplicity of design, and ease of operation compared to other techniques (Chen et al., 2012).

Adsorption has the ability of complete removal of pollutants even from dilute solutions. It also does not result in the formation of harmful substances (Rafatullah et al., 2010). Activated carbon has high adsorption capacity for many pollutants (Altaher and Dietrich, 2014). This is the reason why many adsorption studies have focused on the applications of such material for wastewater treatment (Štrkalj et al., 2013). The major drawbacks of using activated carbon include the high cost of production and problems of regeneration. This has led many researchers to investigate the use of low cost and efficient adsorbents to remove heavy metals and other pollutants from wastewater.

Many materials have been reported as adsorbent for the removal of heavy metals, some of them are, grape stalk (Fiol et al., 2008), coconut (Gonzalez et al., 2008), trunk palm fibers (Altaher et al., 2015), rice shells (Bhattacharya et al., 2008), carbonized Eupatorium adenophorum Spreng (Jin-fa et al., 2018), treated oil palm fibre (Isa et al., 2008), green tea waste (Park et al., 2008), olive stone (Blázquez et al., 2009) seaweeds (Vijayaraghavan et al., 2005), coconut husks (Gupta et al., 2010b), waste rubber tire (Gupta et al., 2012), deoiled mustard (Gupta et al., 2010a), Ficus carica bast (Gupta et al., 2013), polypyrrole (Hasaniet et al., 2015), treated alga (Gupta et al., 2002), rice husk and its ash (Ahmaruzzaman and Gupta, 2011), fertilizer industry waste material (Gupta et al., 2010c), nanoparticles (Predescu et al., 2016), orange peel (Gupta and Nayak, 2012), and carbon nanotubes (Gupta and Saleh, 2013).

In the current study, dates stones (DS) and dates palm fibers (PF); two agricultural wastes from palm trees, were investigated as low-cost adsorbents for the removal of hexavalent chromium ions from aqueous solutions. The experimental parameters that may affect the adsorption process such as initial concentration, temperature, pH, contact time, stirring rate and the adsorbent dose were studied. Some adsorption and kinetic models were applied to investigate the validity of the produced data.

## 2. Materials and methods

### 2.1. Adsorbate

Potassium dichromate stock solution was prepared by dissolving 1 g of the solid pure reagent (weighed to the fourth decimal point) in 1000 mL of distilled water. The working solution was prepared by diluting the stock solution with distilled water to the required concentration. The initial and final concentration of Cr(VI) was determined following ASTM method number (3500 Cr B) based on the reaction of the hexavalent chromium ions with diphenyl carbazide to form a red-violet color that can be measured at a wavelength of 540 nm. Shimadzu UV-Spectrophotometer was utilized for the determination.

### 2.2. Adsorbent

Date stones and palm fibers were obtained from the local market at Yanbu, Saudi Arabia. The samples were washed several times with tap water to remove foreign materials and dust, followed by washing three times with distilled water. The samples were then dried in an oven at 105°C overnight.

The samples were ground into fine powder by a kitchen mixer. The powder was sieved to the required size and kept in sealed glass bottles. No chemical treatment was applied to the two adsorbents.

#### 2.2.1. Characterization of adsorbents

##### 2.2.1.1. Fourier Transform Infrared (FT-IR) study

The FTIR spectra of the two adsorbents were investigated using Infra red Spectrophotometer Varian, USA, FT IR 800 Scimitar Series. The spectra were recorded in the range between 4000 and 400  $\text{cm}^{-1}$  as KBr pellets. The pressed KBr pellets were prepared by grinding 200 mg of adsorbent samples with 0.5 g of KBr.

##### 2.2.1.2. Scanning Electron Microscope (SEM) study

The surface morphology of the two adsorbents was examined using scanning electron microscope [SEM (JEOL-JSM 5300)] at different magnification.

##### 2.2.1.3. Zero point of charge

The zero point of charge (pH<sub>zpc</sub>) was determined by preparing 2 series of flasks containing 0.1N NaCl. One series was intended for DS and the other was for PF. The pHs of the two series were adjusted using NaOH and HCl. A fixed amount of the adsorbent (0.15 g) was added to each flask. The mixtures were shaken for 48 hours at room temperature. The final pH of each solution was determined (Kun-yu et al., 2008).

#### 2.2.1.4. Specific surface area, apparent density, moisture and ash content

The specific surface area was determined by using Sears method (Sears, 1956). According to this method, 1.5 g of the adsorbent was added to 100 mL dilute HCl to reach a pH value in the range 3 - 3.5. Sodium chloride (30 g) was added to the acidic solution with continuous stirring. The mixture volume was made up to 150 mL using distilled water. The suspension was titrated with standard 0.1 M NaOH to reach a pH 4 and then 9. The added volume (V) required to raise the pH from 4 to 9 was recorded. The test was made in triplicate and the value of surface area (S) was determined depending on the average of the three obtained value.

The apparent density of each adsorbent was determined by filling a 10 mL measuring cylinder with the adsorbent. Gentle tapping was applied on the cylinder wall to fill the gaps between adsorbents particles. The apparent density was determined as the mass of the adsorbent required to fill the cylinder divided by the volume of the cylinder.

To determine the moisture content of the adsorbent, 10 grams of the adsorbent (weighed to the fourth decimal point) were placed into weighing watch glass. The watch glass was then placed inside an oven at 105 °C. After 5 hours of drying, the watch glass was cooled in desiccator. The mass of the dried adsorbent was then measured. The average moisture content of the samples was assumed to be the mass loss from the adsorbent sample. The experiment was repeated five times and the average was calculated.

For determination of ash content, three clean empty crucibles were ignited at 550°C for 30 minutes, cooled in a desiccator and then weighed. Accurately weighed 10g of each adsorbent were placed in each crucible. The samples were ignited at 550°C for 2 hours. The difference in weight of crucibles before and after ignition represented the ash content. The experiment was repeated three times and the average was considered.

#### 2.2.1.5. Determination of the functional groups (Boehm's titration)

The surface functional groups of the two adsorbents were determined using Boehm's titration procedure (Boehm, 2002). This method includes acid-base titration of the adsorbent to identify the nature of functional groups on the surface of adsorbent. Twenty-five milli-grams of date stones or palm fibers were placed in 25 ml of 0.1 M solution of each of sodium bicarbonate, sodium carbonate or sodium hydroxide. The mixtures were shaken for 24 h then centrifuged at 6000 rpm. A given amount of each supernatant (5 ml) was titrated with 0.1 M hydrochloric acid solution. Similar procedures were performed with blank samples. Triplicate of this experiment was conducted and the average was calculated. The number of acidic sites was determined under the assumptions that sodium bicarbonate neutralizes carboxylic groups, sodium carbonate neutralizes both carboxylic and lactonic

groups and sodium hydroxide neutralizes carboxylic, lactonic and phenolic groups.

### 2.3. Adsorption equilibrium studies

The adsorbate uptake at equilibrium,  $q_e$  (mg/g), was determined by (Eq. 1).

$$q_e = \frac{(C_o - C_e)V}{W} \quad (1)$$

where  $C_o$  and  $C_e$  (mg/L) are the initial and final concentration of the dye, respectively,  $W$  (g) is the mass of the adsorbent used, and  $V$  (L) is the volume of the solution. Percentage dye removal ( $R$ ) is determined according to (Eq. 2).

$$R = \frac{C_o - C_e}{C_o} \times 100 \quad (2)$$

The adsorbent capacity towards chromium removal (effect of adsorbent mass) was investigated by adding fixed volumes (0.05 L) of the working solution of chromium of known concentration (50 mg/L) to 125 mL conical flasks containing different masses of adsorbent. The flasks were stoppered and shaken for 300 min at a rate of 300 rpm. The solutions were filtered using 0.45  $\mu$ m membrane filters and the residual hexavalent chromium in the filtrate was determined using the diphenyl carbazide method as described before. To investigate the other factors that may affect the adsorption process (pH, initial concentration and time of agitation), the previous procedure was conducted several times. In every experiment all factors were kept constant and the studied factor was changed. All experiments were conducted at room temperature ( $20 \pm 2^\circ\text{C}$ ). Other experimental conditions are summarized in Table 1.

### 2.4. Mathematical models

#### 2.4.1. Adsorption isotherms

The linear form of Langmuir isotherm is given by (Eq. 3).

$$\frac{C_e}{q_e} = \frac{1}{q_m \cdot K_L} + \frac{C_e}{q_m} \quad (3)$$

where  $C_e$  (mg/L) is the equilibrium concentration,  $q_m$  (mg/g) is the maximum adsorption capacity,  $q_e$  (mg/g) is the adsorption capacity at equilibrium, and  $K_L$  (L/mg) is a constant related to adsorption rate. The favorability of the adsorption is determined by the dimensionless separation factor  $R_L$  which is given by (Eq. 4).

$$R_L = \frac{1}{1 + K_L C_o} \quad (4)$$

where  $C_o$  (mg/L) is the initial dye concentration and  $K_L$  is Langmuir constant.

The value of separation factor indicates the favorability of the adsorption process as follows:

**Table 1.** Range of variables for batch experiments

Experiment	Initial concentration, mg/L	Contact time, min	Adsorbent mass, g	Stirring rate, rpm	Particle size, μm	pH	Volume, mL
Effect of initial concentration	15-450	300	0.15	300	< 250	≈4.5	50
Effect of adsorbent mass	50	300	0.05-0.3	300	< 250	≈4.5	50
Effect of time	50	5-360	0.15	300	< 250	≈4.5	50
Effect of pH	50	300	0.15	300	< 250	2-7	50
Effect of temperature 10, 20, 30, 40°C	50	300	0.15	300	< 250	≈4.5	50

Unfavorable ( $R_L > 1$ ), linear ( $R_L = 1$ ), favorable ( $0 < R_L < 1$ ), and irreversible ( $R_L = 0$ ). The linear form of Freundlich model is given by (Eq. 5).

$$\ln q_e = \ln k_f + \frac{1}{n} \ln C_e \tag{5}$$

where  $q_e$  and  $C_e$  have the same definition as Langmuir equation,  $k_f$  ( $\text{mg/g}(\text{mg/L})^{1/n}$ ) is constant related to the bonding energy.  $K_f$  is defined as the adsorption coefficient, and  $1/n$  identifies the adsorption intensity of adsorbate onto adsorbent. If the value of exponent  $n$  is greater than 1, the adsorption represents favorable adsorption conditions.

The linear form of Temkin isotherm is given by Eqs. (6-7).

$$q_e = B_T (\ln K_T) + B_T \ln(C_e) \tag{6}$$

$$B_T = \frac{RT}{b} \tag{7}$$

where  $q_e$  (mg/g) and  $C_e$  (mg/L) have the same definition as in Langmuir equation,  $B_T$  (J/mol) is Temkin isotherm constant related to the heat of adsorption,  $b$  is Temkin isotherm constant,  $R$  is the universal gas constant (8.314 J/mol K), and  $T$  is the absolute temperature (K). The constant  $K_T$  (L/mg) is the equilibrium binding constant, corresponding to maximum binding energy.

Dubinin-Radushkevich model is represented by Eq. (8):

$$\ln q_e = \ln q_m - B\varepsilon^2 \tag{8}$$

where  $q_e$  is the amount of adsorbate adsorbed onto adsorbent surface (mg/g),  $q_m$  represents the maximum adsorption capacity of adsorbent (mg/g), and  $B$  is a constant related to the mean free energy of adsorption per mole of adsorbate.

The Polanyi potential ( $\varepsilon$ ) is given by Eqs. (9-10):

$$\varepsilon = RT \ln\left(1 + \frac{1}{C_e}\right) \tag{9}$$

$$E = \frac{1}{(2B)^{0.5}} \tag{10}$$

$R$  is the universal gas constant in J/mol.  $K$  and  $T$  is the temperature (K).

#### 2.4.2. Kinetic models

Many kinetic models have been introduced to examine the mechanism of adsorption processes. Some of the commonly used kinetic models were applied. These kinetic models are pseudo first order, pseudo second order, Boyd model, intraparticle diffusion model and Elovich equation.

The linear form of pseudo first order model is given by Eq. (11):

$$\ln(q_e - q_t) = \ln q_e - k_1 t \tag{11}$$

where  $q_e$  (mg/g) and  $q_t$  (mg/g) are the amounts of dye adsorbed on the surface of the adsorbate at equilibrium and at any time  $t$  (min), respectively; and  $k_1$  ( $\text{min}^{-1}$ ) is the rate constant of the pseudo first order equation.

The linear form of the pseudo second order model is given by Eq. (12):

$$\frac{t}{q_t} = \frac{1}{k_2 q_m^2} + \frac{t}{q_m} \tag{12}$$

where  $k_2$  (g/mg.min) is the rate constant of the pseudo second order equation,  $q_m$  (mg/g) is the maximum adsorption capacity,  $q_t$  (mg/g) is the amount adsorbed at time  $t$  (min).

Boyd model (Hu et al., 2011) is applied to distinguish between the pore and film diffusion. This model is expressed in Eq. (13):

$$B_t = -0.4977 - \ln(1 - F) \tag{13}$$

where  $B_t$  is the mathematical function of  $F$  and  $F$  represents the fraction of solute adsorbed at time  $t$  (h) and  $F = q_t / q_e$

According to the model, if the plot of  $B_t$  versus  $t$  passes through the origin, pore diffusion is the rate determining step. Otherwise, the adsorption process is film diffusion controlled.

Intraparticle diffusion model considers the intraparticle diffusion as the rate controlling step for adsorption. It is given by Eq. (14):

$$q_t = k_{id} t^{0.5} + C \tag{14}$$

where  $q_t$  (mg/g) is the amount adsorbed at time  $t$  (min) and  $k_{id}$  (mg/g.min<sup>0.5</sup>) is the rate constant for the intraparticle diffusion model.

A simplified linearized form of Elovich equation (Malkoc and Nuhoglu, 2007) can be introduced by Eq. (15):

$$q_t = \frac{1}{B} \ln(\alpha B) + \frac{1}{B} \ln t \quad (15)$$

where  $\alpha$  (mg/g min) is the initial adsorption rate and  $B$  (g/mg) is the adsorption constant related to the extent of the surface coverage and activation energy for chemisorption.

### 2.5. Thermodynamic study

The thermodynamics data obtained from the adsorption process can be used to introduce the adsorption mechanism. The Gibbs free energy change  $\Delta G$  can be calculated by Eq. (16):

$$\Delta G = -RT \ln K_L \quad (16)$$

where  $K_L$  is the Langmuir adsorption constant,  $R$  is the universal gas constant and  $T$  is the absolute temperature. The enthalpy change and the entropy can be obtained from Van't Hoff equation (Eq. 17):

$$\ln K_L = \frac{\Delta S}{R} - \frac{\Delta H}{RT} \quad (17)$$

The enthalpy change and entropy change can be obtained from the slope and intercept of the line obtained by plotting  $\ln K_L$  against  $1/T$ , respectively.

## 3. Results and discussion

### 3.1. Infrared (FTIR) Spectral Analysis

FTIR spectra for both adsorbents are illustrated by Figs. 1a-b. The figures indicate a number of absorption peaks suggesting complex properties of the adsorbents. Spectra are similar for both samples. The peaks in the region 1200–1000 cm<sup>-1</sup> may represent C–O stretching vibrations (Sain and Panthapulakkal, 2006). The band at 1261 cm<sup>-1</sup> in the spectrum of palm fibers is ascribable to the bending modes of O–C–H, C–C–H and C–O–H (Bouchelta et al., 2008). The peaks at 1377 and 1379 cm<sup>-1</sup> are due to C–H bending vibrations. The peaks at 1516, 1523 and 1426, 1441 cm<sup>-1</sup> may be ascribed to C=C stretching of aromatic skeletal mode (Pavan et al., 2008; Sain and Panthapulakkal, 2006). The bands at 1641 and 1631 cm<sup>-1</sup> may represent C=C stretching vibration of alkenes or C=N vibrations in aromatic region. The peak at 1743 cm<sup>-1</sup> in the spectrum of date stones is assigned to C=O stretching vibration of carboxylic groups of lignin and/or hemicelluloses (Pavan et al., 2008; Sun et al., 2005). The bands observed at 2924 and 2860 cm<sup>-1</sup> are assigned to asymmetric and symmetric C–H and symmetric C–H bands, respectively, present in alkyl groups. The

dominant peaks at 3426 and 3430 cm<sup>-1</sup> respectively for palm fibers and date stones, are attributed to O–H stretching vibrations in hydroxyl groups and appears in this lower region where these groups are involved in hydrogen bonds.

The FTIR spectra of date stones and palm fibers waste are in good agreement with the results of Yang (Yang et al., 2007) who studied the characteristics of cellulose, hemicellulose and lignin. This result is in accordance with the composition of lignocellulosic material such as date stones and palm-trees waste, which are essentially composed of cellulose, hemicellulose and lignin (Bouchelta et al., 2008). Consequently, the FTIR results indicate that the biosorbents presented different functional groups such as hydroxyl, carboxyl and carbonyl, which may be potential biosorption sites for the removal of chromium.

### 3.2. Scanning Electron Microscope (SEM)

The results of the scanning electron microscopy are shown in Figs. 2-3. It is quite clear that the morphology of the two adsorbents is quite different except for one feature which is the macropores position. The macropores seem to be on the surface of the two adsorbents.

Also, these macropores are connected to meso and micropores through channels. The surface of DS is very porous and the pores are irregular and have different dimension. Layers of adsorbent can be clearly seen. On the other hand, the surface of PF showed relatively smooth regions. The pores on the surface of PF seem to be more regular and homogeneously distributed all over the surface.

### 3.3. Specific surface area, moisture, ash content and apparent density

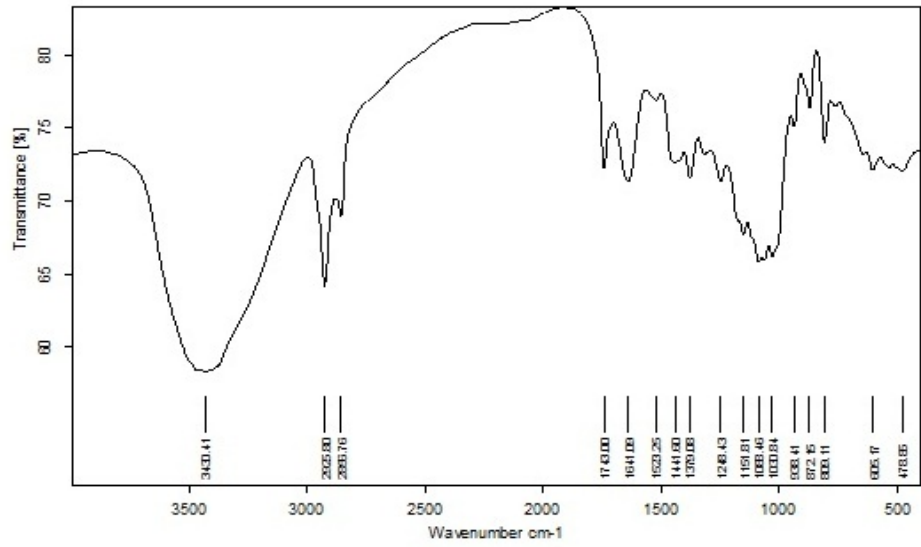
The proximate analyses are shown in Table 2. The percentage moisture content (%MC) was computed as follows (Eq. 18):

$$\%MC = \frac{\text{loss in weight on drying}}{\text{initial mass of sample before drying}} \times 100 \quad (18)$$

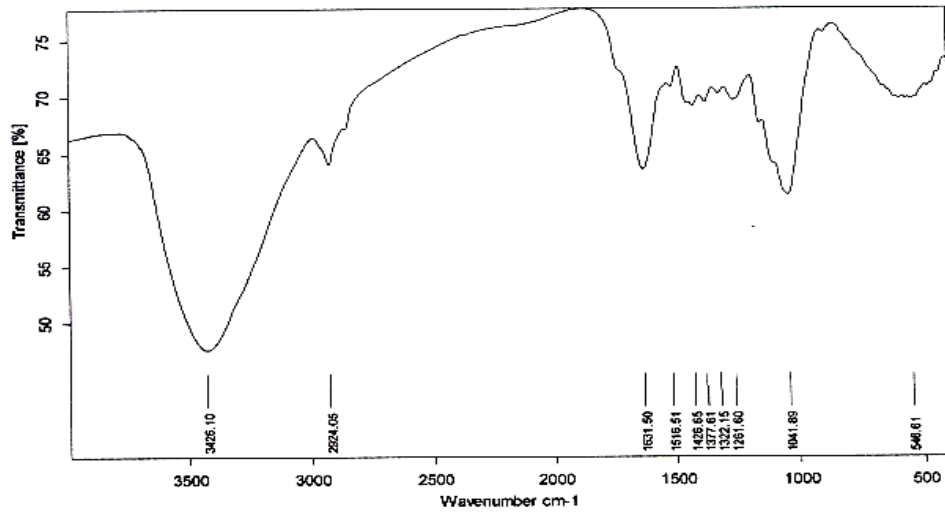
The moisture content is relatively high and indicates the necessity of drying the adsorbent before use or otherwise, taking the moisture content into consideration during calculation. The ash content was calculated using (Eq. 19)

$$\text{Ash content} = \frac{\text{ash weight}}{\text{oven dry weight}} \times 100 \quad (19)$$

Ash content can affect the adsorbent efficiency, i.e. it reduces the overall affinity of adsorbent towards adsorbate. The ash content is low and it indicates that the adsorbent could be used in further studies for production of activated carbon. The specific surface area was calculated using Eq. (20), where  $S$  and  $V$  signification is explained in the section 2.2.1.4.



(a)



(b)

Fig. 1. (a). FTIR spectrum for DS, b. FTIR spectrum for PF

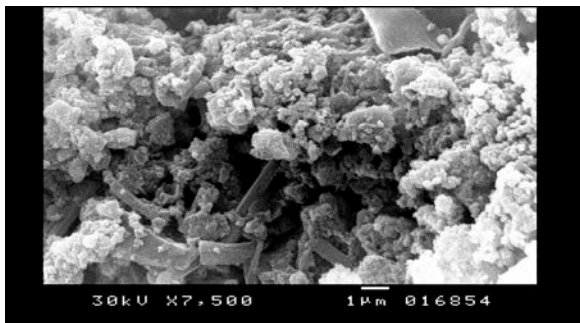


Fig. 2. Scanning electron micrograph of DS

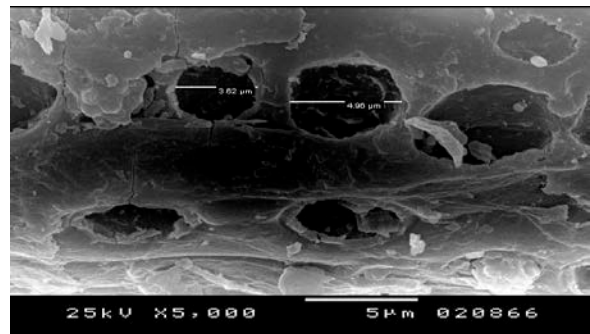


Fig. 3. Scanning electron micrograph of PF

Table 2. Physical properties of adsorbents

<i>Specific surface area, m<sup>2</sup>/g</i>		<i>Ash content, %</i>		<i>Moisture content, %</i>		<i>Apparent density, g/cm<sup>3</sup></i>	
DS	PF	DS	PF	DS	PF	DS	PF
399	237.4	3.19	3.62	3.03	3.3	0.47	0.34

$$S (m^2 g^{-1}) = 32V - 25 \quad (20)$$

The specific area is comparable to many of the agricultural wastes that are commonly used (Ioannidou and Zabaniotou, 2007).

### 3.4. Adsorbent surface functional groups

The results of functional groups distribution on the adsorbent surface are summarized in Table 3. These results are based on Boehm's titration illustrated in previous section. It is well known that surface chemical groups are more complex than shown by Boehm's titration; however, this method gives a semi-quantitative indication about the surface functionalities. It is clear from the results that the acidic sites in both date stones and palm fibers are mainly due to the presence of phenol and carboxyl groups. Few lactones were detected on date stones surface, whereas the palm fiber sample does not contain any lactones.

From the results obtained by the Boehm titration method, it can be observed that the amount of basic groups was significantly higher than total amount of acidic groups. These results suggest that both date stone and palm fibers materials had a basic character.

**Table 3.** Distribution of functional groups on adsorbent surface

Adsorbent	Basic sites, mmol/g	Acidic Sites, mmol/g			
		Carboxyl	Lactone	Phenol	Total acidic sites
Date stones	1.3	0.25	0.10	0.75	1.1
Palm fibers	1.2	0.30	0.00	0.75	1.05

### 3.5. Effect of adsorbent dose on adsorption performance

One very important factor when designing an adsorption system is the optimum adsorbent dose required for this system. Fig. 4 and 5 indicate that increasing the dose of adsorbent increased the adsorption efficiency of adsorbate. Increasing the dose from 1 to 6 g/L resulted in an increase of adsorption removal efficiency from 23 to 69%. However, the adsorption capacity decreased from 11.4 to 5.7 mg/g. On the other hand, for PF, the same increase in adsorbent dose (from 1 – 6 g/L) had a lower effect. The corresponding increase in adsorption removal efficiency was from 15 – 35%. The adsorption capacity for this system increased from 3 – 7.5 mg/g.

These results can be attributed to the effect of the mass of adsorbent on the number of adsorption sites. Increasing the mass of adsorbent increases the number of active sites available for adsorption, thus resulting in increasing removal efficiency.

Another factor that must be taken into consideration is the aggregation of adsorbent particles that may take place due to their high concentration in the solution (high dose of adsorbent in the solution). This aggregation will mask some of the pores on the surface of the adsorbent and also increase the diffusion path length (Ahmaruzzaman, 2008).

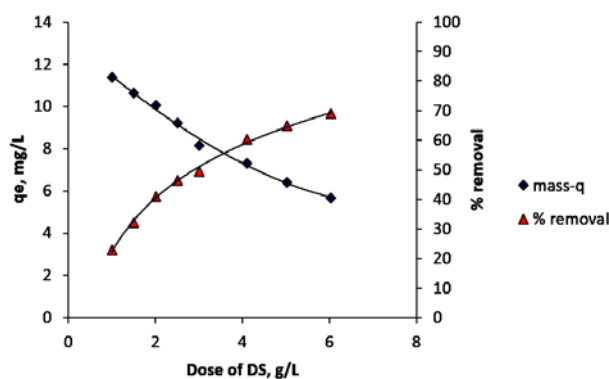


**Fig. 4.** Effect of DS dose on chromium removal

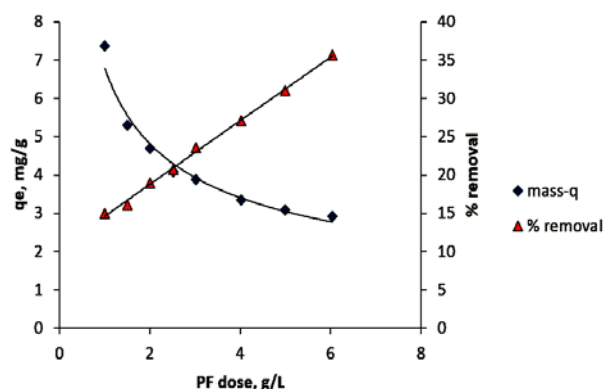


**Fig. 5.** Effect of PF dose on chromium removal

### 3.6. Comparison of adsorption capacity of DP and PF with other adsorbents

The adsorption capacity of Cr (VI) on both dates stones and palm fibers compared with other agricultural wastes adsorbents reported in literature is illustrated in Table 4. It can be noticed that the adsorption capacity of DS (16 mg/g) is higher than some of these adsorbents and similar to others. The adsorption capacity of PF (6 mg/g) is lower than DS and most of the other adsorbents. Many reasons can explain the difference in adsorption capacity among these adsorbents including the difference in specific surface area, the surface functional groups, and the pore size distribution of these adsorbents.

### 3.7. Effect of pH and point of zero charge on adsorption performance

The effect of aqueous solution pH on the adsorption capacity of chromium ion is depicted by Fig. 6.

**Table 4.** Comparison of adsorption capacity of DP and PF with other adsorbents

Adsorbent	Operation conditions					Adsorption capacity, mg/g	Reference
	Adsorbate initial concentration, mg/L	Adsorption time, min	Mass of adsorbent, g/L	Temp. °C	pH		
Saw dust	216	250	5.4	30	1.0	41.5	Gupta and Babu, 2009
Ricinus seed	10	60	50	50	2.0	8.8	Thamilarasu et al., 2012
Pistia stratiotes biomass	10	15	5	40	2.0	7.24	Das et al., 2013
Rice straw	40	1440	10	47	2.0	3.15	Gao et al., 2008
Carnation flowers waste (carnation compost)	10	180	10	18 ± 2	2.0	6.25	Vargas et al., 2012
Date stones	50	300	0.15	20 ± 2	2	16	Present study
Palm fiber	50	300	0.15	20 ± 2	2	6	

As shown in Fig. 6, the adsorption capacity of both DS and PF increased with decreasing the pH of the solution. The highest adsorption capacity was obtained at pH 2. This result is supported by the work of other researchers (Karthikeyan et al., 2005; Malkoc and Nuhoglu, 2007; Sarin and Pant, 2006).

The effect of pH is due to the surface properties of the adsorbent and properties of chromium ions in solution (Jain et al., 2009). Hexavalent chromium may be present in various species in aqueous solutions, e.g.  $H_2CrO_4$ ,  $HCrO_4^-$ ,  $CrO_4^{2-}$  and  $Cr_2O_7^{2-}$  according to the solution pH.

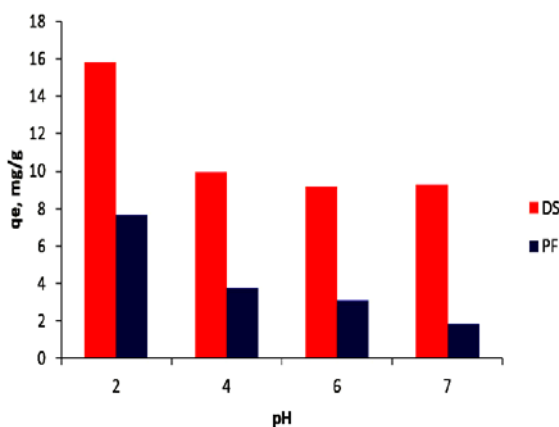


**Fig. 6.** Effect of initial solution pH on chromium removal

The point of zero charge gives a good indication about the surface charge of adsorbent. When the pH of the aqueous solution is below the pH<sub>zpc</sub>, the surface charge of the adsorbent is positive. Meanwhile, the surface of the adsorbent is negatively charged when the pH of the solution is greater than the pH<sub>zpc</sub>. The values of point of zero charge on the surface of DS and PF are 5.5 and 6.5, respectively as illustrated in Fig. 7. These values represent the points at which the initial and final pH values of the system are equal. Below these pH values the surface of the adsorbents will carry

positive charge, while the adsorbate will be present mostly in its anionic form.

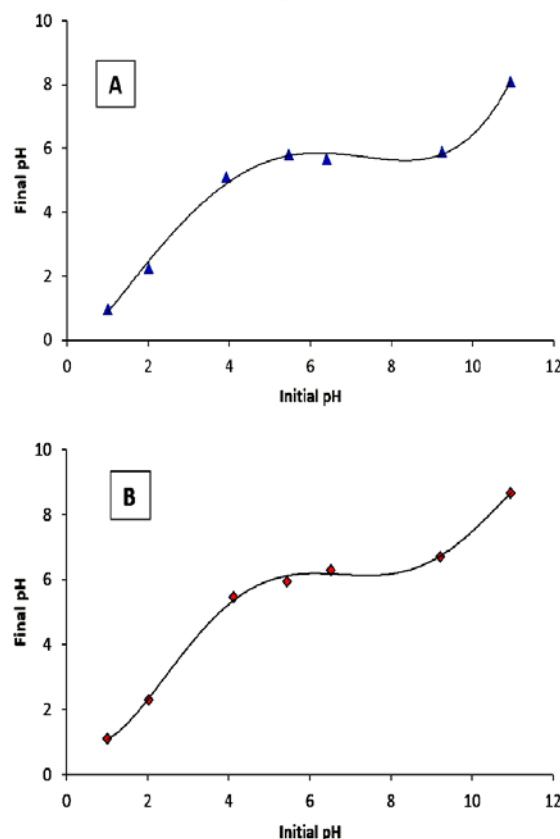


**Fig. 7.** Zero point of charge; A: DS, B: PF

Attraction of these opposite charged species will take place. So, it is expected to have higher adsorption capacity at lower pH. In the pH range 2-6, both  $HCrO_4^-$  and  $Cr_2O_7^{2-}$  species are present in equilibrium. At lower pH ranges,  $Cr_3O_{10}^{2-}$  and  $Cr_4O_{13}^{2-}$  are produced. The adsorption of Cr(VI) may take place through different mechanisms. The electrostatic attraction between the dominant

chromium species ( $HCrO_4^-$ ) present in solution with positively charged sites on the adsorbent is an important mechanism. Chelation with acidic groups on the adsorbent surface and exchange with anions loaded on the residues are two other common mechanisms (Gandhia et al., 2010).

### 3.8. Effect of initial concentration on adsorption

The initial concentration of the metal ion is one of the important factors that may affect the adsorption of metal ions in aqueous solution on the surface of a certain adsorbent. The initial concentration provides the driving force required to overcome the mass transfer resistance of the metal between aqueous solution and solid phase (Aksu and Akpınar, 2000). Fig. 8 illustrates the effect of initial Cr(VI) concentration on the adsorption into both adsorbents. For DS, the adsorption capacity increased from 1.99 mg/g to 74.5 mg/g when increasing the initial concentration from 15 to 450 mg/L. For PF, the increase was from 0.93 mg/g to 62.6 mg/g for the same concentration range.

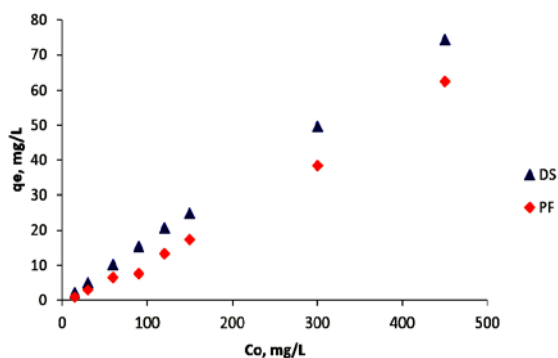


**Fig. 8.** Effect of initial concentration on chromium removal, contact time 300 min, adsorbent mass 0.15 g, stirring rate 300 rpm, particle size < 250  $\mu$ m

For a fixed adsorbent dose, the number of active adsorption sites to accommodate adsorbate ions remains unchanged but with increasing adsorbate concentration, the adsorbate ions to be accommodated increases and hence many of the sites available for adsorption will be occupied. It can be noticed from the figure that adsorption saturation was not reached due to high availability of free adsorption sites on both adsorbents compared to the number of chromium species to be adsorbed. The increase in adsorption capacity accompanied by the increase in initial ion concentration indicates increasing occupation of available binding sites. As was stated before, the initial concentration provides an important driving force to overcome all mass transfer resistances of all molecules between the aqueous and adsorbents. Another effect of high initial concentration of the adsorbate molecules is the probable increase of contact between chromium molecules and adsorbent particles. Some factors must be taken into account when studying the effect of initial ion concentration. First, some of the active

adsorption sites are not occupied by adsorbate molecules which lead to less adsorption capacity. Second, aggregation of the adsorbent particles may take place which lead masking of some of the adsorption sites, thus decreasing the total surface area of the adsorbent in the solution (Yasemin and Tez, 2007).

### 3.9. Adsorption equilibrium

The experimental data were tested with adsorption models namely Langmuir, Freundlich, Temkin and D-R. The characteristic parameters from the slope and intercept of the plots are determined using regression analysis. The parameters are reported in Table 5. The dimensionless separation factor  $R_L$  values (calculated according to Langmuir model) for both DS and PF systems, being less than unity, indicate that adsorption of Cr(VI) on both adsorbents to be favorable. The maximum adsorption capacity of DS is much higher than PF. However, their values are not consistent with the experimental values as indicated by the relatively low  $R^2$  for both adsorbents.

Freundlich is an empirical expression. It assumes that adsorption takes place on multilayers on the surface of adsorbent. As illustrated by the results in Table 5, the Freundlich model fits the data for both DS and PF systems better than the Langmuir model, this is demonstrated by high correlation coefficient ( $R^2$ ) for the data obtained from Freundlich model. The value of  $1/n$  for DS is 0.772 which indicates high favorability of the adsorption of Cr(VI) on DS. On the other hand,  $1/n$  value in case of PF system is 0.362. Comparing these results indicates that the DS adsorption system is more favorable than PF adsorption system. Analysis of the adsorption data using D-R model has a significant importance. It gives an indication about the nature of the adsorption process; physical or chemical.

The mean adsorption energy of the D-R model gives information about the nature of the adsorption process; physical or chemical. If  $E < 8$  kJ/mol, the adsorption process is physical, and if  $8 < E < 16$ , the adsorption process is ion exchange, and if  $E > 16$  kJ/mol the adsorption process is chemical. As indicated in Table 5, the correlation coefficients of adsorption system for DS and PF are high (0.989 and 0.957 for DS and PF, respectively). The maximum adsorption capacity for DS is 15.441 mg/g and that for PF is 21.22 mg/g. The first value agrees well with experimental data, while the other one is not consistent. The  $E$  values being less than 8 kJ/mol suggest the physical adsorption to be the mechanism of adsorption.

Temkin isotherm fits well to the experimental data as indicated by correlation coefficients. Its constants are given in Table 5. The Temkin adsorption potential,  $K_T$ , of DS is 0.159 compared to 0.034 for PF indicating a lower PF-metal ion potential than DS.

**Table 5.** Adsorption parameters for the applied adsorption models

Isotherm		Parameters	Adsorbent	
			DS	PF
Langmuir	20 °C	$R^2$	0.916	0.929
		$q_m$ , mg/g	35.7	2.24
		$K_L$ , L/mg	0.013	0.017
		$R_L$	0.61	0.547
Freundlich	20 °C	$R^2$	0.986	0.955
		$n$	1.295	0.362
		$K_f$ (mg/g)(mg/L) $^{1/n}$	0.71	$1.7 \times 10^{-4}$
Temkin	20 °C	$R^2$	0.997	0.923
		$B_T$ , mg/g	6.385	11.07
		$K_T$ , L/mg	0.159	0.034
Dubinin-Radushkevich	20 °C	$R^2$	0.989	0.957
		$q_m$ , mg/g	15.441	21.22
		$E$ , kJ/mol	0.1	0.016

This is probably due to the difference in pore diameter and pore shape of both adsorbents. As it is depicted by Figs. 2-3, the shape of the DS pores is irregular in contrast to the regular shape of PF pores. The pore radius must be close to the ionic radius for adsorption to take place. The Temkin constants,  $b$  related to heat of sorption for DS and PF are 0.381 and 0.22 kJ/mol, respectively. It has been reported that the typical range of bonding energy for ion-exchange mechanism is 8-16 kJ/mol (Kiran and Kaushik, 2008). The low values in this study indicates a weak interaction between sorbate and sorbent, supporting a physical adsorption mechanism. This result is in agreement with that obtained from D-R isotherm.

### 3.10. Kinetic study

Adsorption kinetics describes the solute uptake rate, which governs the residence time of sorption reaction. It also describes the reaction pathway along times until reaching equilibrium. Fig. 9 depicts the adsorption rate of hexavalent chromium ions on both DS and PF. The adsorption of chromium ions on both DS and PF displays a fast adsorption rate.

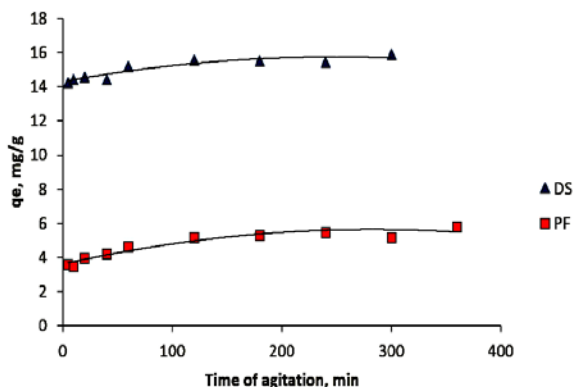


**Fig. 9.** Effect of contact time on the adsorption of chromium on DS and PF

For both adsorbents equilibrium is reached within the first two hours. The adsorption took place in two different stages. The first one was very fast. This is illustrated by the fact that for DS, 86 % of the chromium ions was removed within the first 10 min (maximum removal efficiency was 94%). The next stage was a slow stage ending with equilibrium. A similar behavior could be observed for PF. Within the first 10 min, 21 of the chromium ions were removed compared to 34% removal efficiency at equilibrium. The rapid uptake of the metal ions at the early stage of the adsorption process may be attributed to the availability of active adsorption sites on the adsorbent surface. With time, these sites got occupied and the remaining adsorbate ions would compete for the remaining unoccupied sites which results in slower adsorption rate (Ozdes et al., 2011). Another reason is the concentration gradient. As was mentioned before the high initial concentrations provide a driving force for chromium ions adsorption. At early stages, a great concentration gradient is present between the adsorbate in the bulk of solution and on the surface of adsorbent which easily overcomes the mass transfer resistance. With time, the concentration gradient decreases which decrease the driving force. The kinetic data were evaluated using pseudo-first and second order models. The results of fitting the experimental data to the model are illustrated in Table 6. The data in the table shows that the experimental data had its best fit with the pseudo second order model with higher  $R^2$  value (0.999 and 0.995 for DS and PF, respectively) compared with pseudo first order.

Furthermore, the values of  $q_t$  predicted by the model agree closely with those determined experimentally. Therefore, it can be concluded that the rate of hexavalent chromium ions adsorption is influenced by both the metal ion concentration and adsorbent dose (Abramian and El-Rassy, 2009). The prediction of the rate controlling mechanism is important in adsorption processes since it affects the design and scale-up of the adsorption system. The adsorption process in an aqueous solution is

characterized by either external mass or intraparticle diffusion or both.

**Table 6.** Kinetic parameters for adsorption of chromium on DS and PF

Kinetic model	Parameters	Adsorbate	
		DS	PF
Pseudo first order	$R^2$	0.619	0.503
	$K_1$	0.029	0.026
	$q_m$	5.474	7.374
Pseudo second order	$R^2$	0.999	0.995
	$K_2$	0.032	0.018
	$q_m$	15.873	5.714
Elovich	$R^2$	0.984	0.947
	$B$	2.513	1.835
	$a$	2.31	46.64
Intraparticle diffusion	$R^2$	0.958	0.91
	$K_{id}$	0.104	0.131
	$C$	14.14	3.387
Boyd	$R^2$	0.956	0.88

Since the solution containing the adsorbent is vigorously agitated during the adsorption period, it can be assumed that the rate of adsorption is not affected by mass transfer of ions from the bulk liquid to the particle external surface. In this case, the rate limiting step may be either film or intraparticle diffusion (Moussavi and Khosravi, 2011). As they act in series, the slower of the two will be the rate-determining step. Film diffusion was analyzed using Eq. (13). The plot of liquid film diffusion on both DS and PF is illustrated in Fig. 10. Examining this Figure indicates that two distinct regions can be identified for the two adsorbents. This suggests that two different mechanisms are involved at different intervals. The results show that the film diffusion is not the sole limiting step. The intraparticle diffusion may also be involved in controlling the adsorption process.

To gain further insight into the adsorption behavior the kinetic results were analyzed by intraparticle diffusion model. The fitting of the experimental data to this model was examined by applying Eq. (14). If the intraparticle diffusion is involved in the adsorption process, the plot of the adsorption capacity at any time ( $q_t$ , mg/g) against  $t$  (min) should give a straight line. If the intraparticle diffusion is the only rate controlling mechanism, the straight line should pass through the origin. If the line does not pass through the origin other mechanism may be involved in the adsorption process. The intercepts ( $c$ ) of the produced straight line gives an indication about the thickness of the boundary layer.

The larger the intercept, the greater is the boundary layer effect. As illustrated in Fig. 11, the adsorption on both DS and PF can be represented by straight line according to this mode. Experimental data followed a linear distribution with high correlation coefficient ( $R^2$  values are 0.958 and 0.91 for DS and PF, respectively). The value of the intercept in case of DS system is much greater than that of PF, indicating the great effect of boundary

layer for the former. These results support the finding obtained before from fitting the data to film diffusion model.

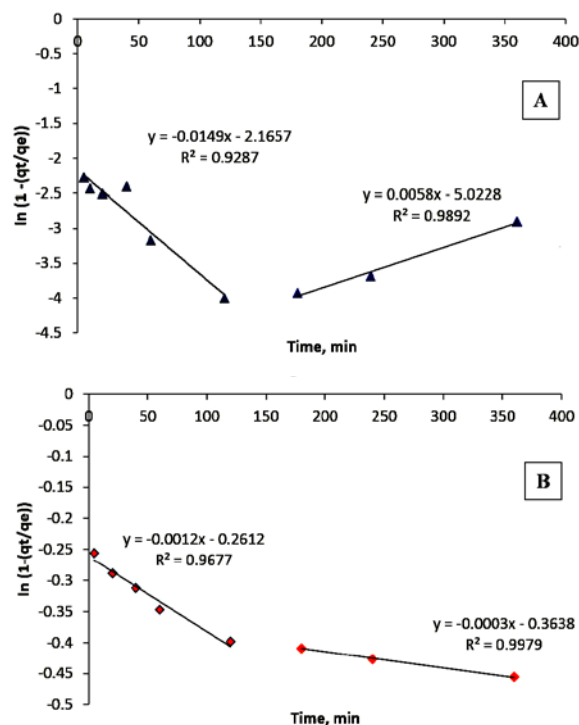


**Fig. 10.** Liquid film diffusion (Boyd model) representation of adsorption of chromium; A: DS, B: PF

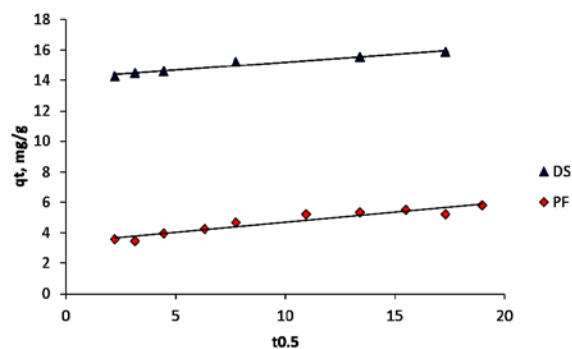


**Fig. 11.** Intraparticle diffusion representation of adsorption of chromium on both DS and PF

The Elovich equation is useful in describing adsorption on heterogeneous surfaces. However, it does not predict any mechanism. If the experimental data fits well to this model that indicates the heterogeneity of adsorbent surface. The data for both DS and PF fit the model very well according to the high correlation coefficient (Table 6 and Fig. 12). This proves the heterogeneity of surfaces of the two adsorbents.

### 3.11. Effect of temperature and thermodynamics of adsorption

Temperature has an important effect on the adsorption process. The increase of solution

temperature will decrease the viscosity of the aqueous solution containing chromium ions.

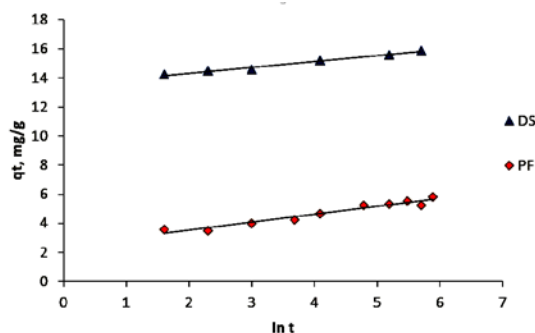


Fig. 12. Elovich model for adsorption of chromium on both DS and PF

This will result in increasing the rate of adsorbate diffusion across the external boundary layer and in the internal pores of the adsorbent. Temperature may also affect the equilibrium of the adsorbate depending on the nature of the adsorption process; whether it is endothermic or exothermic. Finally, it has an effect on the stability of the metal ion species initially placed in solution.

The adsorption capacity increased from 6.803 mg/g to 28.6 mg/g for DS and from 0.062 mg/g to 5.16 mg/g for PF (Figures not shown) when the temperature was increased from 10 to 40°C, indicating that the adsorption process is endothermic in nature for both adsorbents.

The thermodynamic parameters  $\Delta H$  and  $\Delta S$  are introduced in Table 7. These data were calculated from the slope and intercept of the plot between  $\ln K_c$  and  $1/T$ . The values of  $\Delta G$  indicate the favorability of physical adsorption. The positive values of  $\Delta H$  indicate the endothermic nature of adsorption and this governs the possibility of physical adsorption which was also supported by the increase in adsorption capacity with increasing temperature. The negative values of  $\Delta G$  in case of adsorption on DS suggest the high favorability of Cr(VI) adsorption on DS. They also indicate that the metal ion adsorption was spontaneous. On the other hand, the positive values of  $\Delta G$  in case of PF system indicate that this adsorption system is less favorable. Furthermore, the low values of  $\Delta G$  suggest physical adsorption (Kumar and Kirthika, 2009).

Table 7. Thermodynamic parameters of Cr(VI) adsorption onto DS and PF

	T (K)	$\Delta G$ (kJ/mol)	$\Delta H$ (kJ/mol)	$\Delta S$ (J/mol.K)
Dates stones	283	0.71	31.06	108
	293	-2.54		
	303	-2.03		
	313	-2.33		
Palm fiber	283	4.67	33.61	102.6
	293	0.4		
	303	2.1		
	313	1.6		

The positive values of  $\Delta S$  may suggest that Cr(VI) ions replace some water molecules from the solution previously adsorbed on the surface of adsorbent. These displaced molecules gain more translation entropy than is lost by the adsorbate ions, thus allowing the prevalence of randomness in the system. The positive values of  $\Delta S$  may also show the increased disorder and randomness at the solid solution interface during the adsorption process for both systems. In addition, the positive value of  $\Delta S$  reflects the affinity of the adsorbents for the Cr(VI) ions (Najm and Yassin, 2009).

### 3.12. Feasibility study

The two agricultural wastes used in this study are widely available with low cost. These two substances have no significant industrial and commercial uses but become an issue and contribute to environmental problems. Hence, the utilization of such agriculture solid waste for wastewater treatment is beneficial. The alternative of using agricultural waste as adsorbent is activated carbon. Activated carbon has better adsorptivity but its cost of production is very high.

Dates stones collected from dates processing plant are given away for free. Its use in other purposes is negligible. The cost of processing including transportation, washing, drying, crushing, sieving, and labor is SR 200/ton. No chemical treatment is required for its processing. PF is collected during the trimming the palm tree. It is less available. However, its cost of processing is less; SR 100/ton. Compared with the cheapest commercial activated carbon available in the local market (SR 4000/ton), the two adsorbents studied are very good replacement.

### 4. Conclusions

This study indicates that DS has a better adsorption capacity to hexavalent chromium than PF. The adsorption of Cr(VI) on both DS and PF was found to be pH-dependent. The highest removal efficiency was obtained at pH 2. The initial concentration of the metal ion in solution was found to have a pronounced effect on the adsorption process. Increasing the initial concentration resulted in higher adsorption capacity. Freundlich model was found to be the best adsorption equilibrium model that can interpret the experimental data.

The mechanism of adsorption involves both liquid film diffusion and intraparticle diffusion as the rate determining mechanisms. It can be concluded from the results demonstrated here that DS is a potential effective adsorbent for removal of Cr(VI) from aqueous solutions.

### References

Abramian L., El-Rassy H., (2009), Adsorption kinetics and thermodynamics of azo-dyes orange II onto highly

- porous titania aerogel, *Chemical Engineering Journal*, **150**, 403-410.
- Ahmaruzzaman M.D., (2008), Adsorption of phenolic compounds on low cost adsorbents: A review, *Advances in Colloid and Interface Science*, **143**, 48-76.
- Ahmaruzzaman M., Gupta V.K., (2011), Rice husk and its ash as low-cost adsorbents in water and wastewater treatment, *Industrial & Engineering Chemistry Research*, **50**, 13589-13613.
- Aksu Z., Akpınar D., (2000), Modeling of simultaneous biosorption of phenol and nickel (II) onto dried aerobic activated sludge, *Separation and Purification Technology*, **21**, 87-99.
- Altaher H., Dietrich A.M., (2014), Characterizing o-and p-nitrophenols adsorption onto innovative activated carbon prepared from date pits, *Water Science and Technology*, **69**, 31-37.
- Altaher H., Alghamdi A., Omar W., (2015), Innovative biosorbent for the removal of cadmium Ions from wastewater, *Environmental Engineering and Management Journal*, **14**, 793-800.
- Attia A.A., Khedr S.A., Elkholy S.A., (2010), Adsorption of chromium ion (VI) by acid activated carbon, *Brazilian Journal of Chemical Engineering*, **27**, 183-193.
- Bhattacharya A.K., Naiya T.K., Mandal S.N., Das S.K., (2008), Adsorption, kinetics and equilibrium studies on removal of Cr(VI) from aqueous solutions using different low-cost adsorbents, *Chemical Engineering Journal*, **137**, 529-541.
- Blázquez G., Hernáinz F., Calero M., Martín-Lara M.A., Tenorio G., (2009), The effect of pH on the biosorption of Cr (III) and Cr (VI) with olive stone, *Chemical Engineering Journal*, **148**, 473-479.
- Boehm H., (2002), Surface oxides on carbon and their analysis: a critical assessment, *Carbon*, **40**, 145-149.
- Bouchelta C., Medjram M.S., Bertrand O., Bellat J.P., (2008), Preparation and characterization of activated carbon from date stones by physical activation with steam, *Journal of Analytical and Applied Pyrolysis*, **82**, 70-77.
- Chen C., Zhang M., Guan Q., Li W., (2012), Kinetic and thermodynamic studies on the adsorption of xylenol orange onto MIL-101(Cr), *Chemical Engineering Journal*, **183**, 60-67.
- Das B., Mondal N.K., Roy P., Chattaraj S., (2013), Equilibrium, kinetic and thermodynamic study on chromium(VI) removal from aqueous solution using *Pistia Stratiotes* biomass, *Chemical Science Transaction*, **2**, 85-104.
- Fathima A., Sadiq M., Rao J.R., Nair B.U., (2016), Bioremoval of trivalent chromium using indigenous bacillus species– a biofilm based approach, *Environmental Engineering and Management Journal*, **15**, 1603-160.
- Fiol N., Escudero C., Villaescusa I., (2008), Chromium sorption and Cr(VI) reduction to Cr(III) by grape stalks and yohimbe bark, *Bioresource Technology*, **99**, 5030-5036.
- Gandhia M.R., Viswanathan N., Meenakshi S., (2010), Adsorption mechanism of hexavalent chromium removal using Amberlite IRA 743 resin, *Ion Exchange Letters*, **3**, 25-35.
- Gao H., Liu Y., Zeng G., Xu W., Li T., Xia W., (2008), Characterization of Cr(VI) removal from aqueous solutions by a surplus agricultural waste-rice straw, *Journal of Hazardous Materials*, **150**, 446-452.
- Gheju M., Balcu I., (2011), Removal of chromium from Cr(VI) polluted wastewaters by reduction with scrap iron and subsequent precipitation of resulted cations, *Journal of Hazardous Materials*, **196**, 131-138.
- Ghorbani F., Younesi H., (2016), Bioremediation of chromium (VI) from aqueous solution by *Aspergillus niger*: optimization of process parameters, *Environmental Engineering and Management Journal*, **15**, 2551-2558.
- Gonzalez M.H., Araujo G.C., Pelizaro C.B., Menezes E.A., Lemos S.G., de Sousa G.B., Nogueira A.R., (2008), Coconut coir as biosorbent for Cr(VI) removal from laboratory wastewater, *Journal of Hazardous Materials*, **159**, 252-256.
- Gupta S., Babu V., (2009), Removal of toxic metal Cr(VI) from aqueous solutions using sawdust as adsorbent: Equilibrium, kinetics and regeneration studies, *Chemical Engineering Journal*, **150**, 352-365.
- Gupta V.K., Ganjali M.R., Nayak A., Bhushan B., Agarwal S., (2012), Enhanced heavy metals removal and recovery by mesoporous adsorbent prepared from waste rubber tire, *Chemical Engineering Journal*, **197**, 330-342.
- Gupta V.K., Jain R., Malathi S., Nayak A., (2010a), Adsorption-desorption studies of indigocarmine from industrial effluents by using deoiled mustard and its comparison with charcoal, *Journal of colloid and interface science*, **348**, 628-633.
- Gupta V.K., Jain R., Shrivastava M., Nayak A., (2010b), Equilibrium and thermodynamic studies on the adsorption of the dye Tartrazine onto waste “Coconut Husks” carbon and activated Carbon, *Journal of Chemical & Engineering Data*, **55**, 5083-5090.
- Gupta V.K., Nayak A., (2012), Cadmium removal and recovery from aqueous solutions by novel adsorbents prepared from orange peel and Fe<sub>2</sub>O<sub>3</sub> nanoparticles, *Chemical Engineering Journal*, **180**, 81-90.
- Gupta V.K., Pathania D., Agarwal S., Sharma S., (2013), Removal of Cr (VI) onto *Ficus carica* biosorbent from water, *Environmental Science and Pollution Research*, **20**, 2632-2644.
- Gupta V.K., Rastogi A., Nayak A., (2002), Biosorption of nickel onto treated alga (*Oedogonium hatei*): Application of isotherm and kinetic models, *Journal of Colloid and Interface Science*, **342**, 533-539.
- Gupta V.K., Rastogi A., Nayak A., (2010c), Adsorption studies on the removal of hexavalent chromium from aqueous solution using a low-cost fertilizer industry waste material, *Journal of Colloid and Interface Science*, **342**, 135-141.
- Gupta V.K., Saleh T.A., (2013), Sorption of pollutants by porous carbon, carbon nanotubes and fullerene-An overview, *Environmental Science and Pollution Research*, **20**, 2828-2843.
- Hasani E., Farnam M., Asl S.M.H., Reza Katal , Rastegar S.O., (2015), Batch and column removal of chromium (VI) from aqueous solution using polypyrrole, *Environmental Engineering and Management Journal*, **14**, 17-28.
- Hlihor R.M., Apostol L.C., Smaranda C., Pavel L.V., Caliman F.A., Robu B.M., Gavrilescu M., (2009), Bioavailability processes for contaminants in soils and their use in risk assessment, *Environmental Engineering and Management Journal*, **8**, 1199-1206.
- Hu X.J., Wang J.S., Liu Y.G., Li X., Zeng G.M., Bao Z.L., Zeng X.X., Chen A.W., Long F., (2011), Adsorption of chromium (VI) by ethylenediamine-modified cross-linked magnetic chitosan resin: Isotherms, kinetics and

- thermodynamics, *Journal of Hazardous Materials*, **185**, 306-314.
- Ioannidou O., Zabaniotou A., (2007), Agricultural residues as precursors for activated carbon production-A review, *Renewable and Sustainable Energy Reviews*, **11**, 1966-2005.
- Isa M.H., Ibrahim N., Aziz H.A., Adlan M.N., Sabiani N.H.M., Zinatizadeh A.A.L., Kutty S.R.M., (2008), Removal of chromium (VI) from aqueous solution using treated oil palm fibre, *Journal of Hazardous Materials*, **152**, 662-668.
- Jin-fa C., Yong G., Da-gang S., Sha Y., (2018), Adsorption characteristics of Cr (VI) on a carbonized Eupatorium adenophorum SPRENG, *Environmental Engineering and Management Journal*, **17**, 115-122.
- Jain M., Garga V.K., Kadirvelu K., (2009), Chromium (VI) removal from aqueous system using *Helianthus annuus* (sunflower) stem waste, *Journal of Hazardous Materials*, **162**, 365-372.
- Karthikeyan T., Rajgopal S., Miranda L.R., (2005), Chromium (VI) adsorption from aqueous solution by *Hevea brasiliensis* sawdust activated carbon, *Journal of Hazardous Materials*, **B124**, 192-199.
- Kiran B., Kaushik A., (2008), Chromium binding capacity of *Lyngbya putealis* exopolysaccharides, *Biochemical Engineering Journal*, **38**, 47-54.
- Kumar P.S., Kirthika K., (2009), Equilibrium and kinetic study of adsorption of nickel from aqueous solution onto bael tree leaf powder, *Journal of Engineering Science and Technology*, **4**, 351-363.
- Kun-yu Z., Hui-ping H., Li-juan Z., AQi-yuan C., (2008), Surface charge properties of red mud particles generated from Chinese diaspore bauxite, *Transaction of Nonferrous Metals Society of China*, **18**, 1285-1289.
- Malkoc E., Nuhoglu Y., (2007), Determination of kinetic and equilibrium parameters of the batch adsorption of Cr(VI) onto waste acorn of *Quercus ithaburensis*, *Chemical Engineering and Processing*, **46**, 1020-1029.
- Moussavi G., Khosravi R., (2011), The removal of cationic dyes from aqueous solutions by adsorption onto pistachio hull waste, *Chemical Engineering Research and Design*, **89**, 2182-2189.
- Najm T., Yassin S., (2009), Removal of chromium from aqueous solution using modified pomegranate peel: mechanistic and thermodynamic studies, *E-journal of Chemistry*, **6**, S153-S158.
- Natarajan B., Nagarajan S., (2010), Utilisation of agriculture weed for the removal of Cr(VI) from aqueous solution, *Acta Chimica Slovenica*, **57**, 693-699.
- Ozdes D., Duran C., Senturk H.B., (2011), Adsorptive removal of Cd(II) and Pb(II) ions from aqueous solutions bu using Turkish illitic clay, *Journal of Environmental Management*, **92**, 3082-3090.
- Park D., Lim S.L., Yun Y.S., Park J.M., (2008), Development of a new Cr (VI)-biosorbent from agricultural biowaste, *Bioresource Technology*, **99**, 8810-8818.
- Pavan F.A., Lima E.C., Dias S.L.P., Mazzocato A.C., (2008), Methylene blue biosorption from aqueous solutions by yellow passion fruit waste, *Journal of Hazardous Materials*, **150**, 703-712.
- Predescu A. Matei E., Predescu A., Berbecaru A., Sohaciu M., Predescu C., (2016), Removal of hexavalent chromium from waters by means of a TiO<sub>2</sub>-Fe<sub>3</sub>O<sub>4</sub> nanocomposite, *Environmental Engineering and Management Journal*, **15**, 989-994.
- Rafatullah M., Sulaiman O., Hashim R., Ahmad A., (2010), Adsorption of methylene blue on low-cost adsorbents: a review, *Journal of Hazardous Materials*, **177**, 70-80.
- Sain M., Panthapulakkal S., (2006), Bioprocess preparation of wheat straw fibers and their characterization, *Industrial Crops and Products*, **23**, 1-8.
- Sarin V., Pant K.K., (2006), Removal of chromium from industrial wastewater by using eucalyptus bark, *Bioresource Technology*, **97**, 15-20.
- Sears G.W., (1956), Determination of specific surface area of colloidal silica by titration with sodium hydroxide, *Analytical Chemistry*, **28**, 1981-1983.
- Sadeghi S., Moghaddam M.R., Arami M., (2017), Techno-economical evaluation of hexavalent chromium removal by electrocoagulation process with the aid of polyaluminum chloride as coagulant: optimization through response surface methodology, *Environmental Engineering and Management Journal*, **16**, 93-104.
- Štrkalj A., Glavaš Z., Brnardić I., (2013), Application of foundry waste for adsorption of hexavalent chromium, *Chemical and Biochemical Engineering*, **27**, 15-19.
- Sun X.F., Xu F., Sun R.C., Fowler P., Baird M.S., (2005), Characteristics of degraded cellulose obtained from steam-exploded wheat straw, *Carbohydrate Research*, **340**, 97-106.
- Thamilarasu P., Sharmila R., Karunakaran K., (2012), Kinetic, equilibrium and thermodynamic studies on removal of Cr(VI) by modified activated carbon prepared from *Ricinus communis* seed shell, *Coromandal Journal of Science*, **1**, 30-39.
- Vargas C., Brandã P.F.B., Ágrede J., Castillo E., (2012), Bioadsorption using compost: An alternative for removal of chromium (VI) from aqueous solutions, *BioResources*, **7**, 2711-2727.
- Vijayaraghavan K., Jegan J., Palanivelu K., Velan M., (2005), Biosorption of cobalt (II) and nickel (II) by seaweeds: batch and column studies, *Separation and Purification Technology*, **44**, 53-59.
- Yang H., Yan R., Chen H., Lee D.H., Zheng C., (2007), Characteristics of hemicellulose, cellulose and lignin pyrolysis, *Fuel*, **86**, 1781-1788.
- Yasemin B., Tez Z., (2007), Adsorption studies on ground shells of hazelnut and almond, *Journal of Hazardous Materials*, **149**, 35-41.